Since January 2020 Elsevier has created a COVID-19 resource centre with free information in English and Mandarin on the novel coronavirus COVID-19. The COVID-19 resource centre is hosted on Elsevier Connect, the company's public news and information website.

Available online at www.sciencedirect.com

ScienceDirect

IFAC PapersOnline CONFERENCE PAPER ARCHIVE

IFAC PapersOnLine 54-20 (2021) 251–257

Estimation of the Basic Reproduction Number for the COVID-19 Pandemic in Minnesota

H. Movahedi*, A. Zemouche, R. Rajamani*****

** University of Minnesota, Twin Cities, Minneapolis, MN 55455, USA (e-mail: movah007@umn.edu, PIN: 116365).*

*** University of Lorraine, IUT Henri Poincaré de Longwy, CRAN CNRS UMR 7039, 54400 Cosnes et Romain, France (email: ali.zemouche@univ-lorraine.fr, PIN: 59252)*

**** University of Minnesota, Twin Cities, Minneapolis, MN 55455, USA (e-mail: rajamani@umn.edu, PIN: 24626), Corresponding author*

Abstract: This paper focuses on the dynamics of the COVID-19 pandemic and estimation of associated real-time variables characterizing disease spread. A nonlinear dynamic model is developed which enhances the traditional SEIR epidemic model to include additional variables of hospitalizations, ICU admissions, and deaths. A 6-month data set containing Minnesota data on infections, hospital-ICU admissions and deaths is used to find least-squares solutions to the parameters of the model. The model is found to fit the measured data accurately. Subsequently, a cascaded observer is developed to find real-time values of the infected population, the infection rate, and the basic reproduction number. The observer is found to yield good real-time estimates that match the least-squares parameters obtained from the complete data set. The importance of the work is that it enables real-time estimation of the basic reproduction number which is a key variable for controlling disease spread.

Keywords: COVID-19, Infectious disease, Observers, Nonlinear dynamics, Estimation in biological systems, Basic reproduction number

1. INTRODUCTION

The COVID-19 infections were first reported in December 2019 in Wuhan, China and subsequently spread rapidly around the world. The successful development of vaccines in recent months promises an eventual recovery for the world from the disease. However, mutations of the involved SARS-Cov-2 virus still present an unknown danger. Furthermore, the world has experienced a significant number of other infectious viral outbreaks during the last 20 years, including the SARS, MERS, and Ebola epidemics (De Wit et al, 2016). Hence, there is significant motivation to understand the dynamics of how these diseases spread in populations and to develop techniques to control their spread (Chen, & Sun, 2014; De la Sen et al, 2017).

A number of research articles have recently explored development of mathematical models to represent the dynamics of different agents involved in the spread of the COVID-19 disease. The models attempt to describe the evolution of infected numbers of the population, as well as hospitalized, recovered and susceptible numbers. Most models are compartmental models, also known as *SIR* models, based on an assumption that the population size is constant (Zhong et al, 2020). Members of the population are classified into three compartments, namely *S*-susceptible, *I*-infected and *R*-removed. Susceptible people are those lacking immunity and therefore susceptible but not yet infected. An individual in group *S* can move to group *I* by infection possibly caused by proximity to an infected individual. Finally, an infected individual fully recovered from the disease or deceased will be moved from the group *I* to the group *R*. The summation of these three compartments in the SIR model remains constant and equals the total population *N*. An improvement on the SIR model is the SEIR model (Hethcote, & Van den Driessche, 1991). In the SEIR model a fourth group denoted as Exposed (*E*) is added as a transition group between the groups *S* and *I*. The *E* group is the population that has been infected with the virus but is not yet in an infectious stage capable of transmitting the virus to others. The addition of the compartment *E* has been shown to improve model accuracy in data from a number of epidemics (Lopman et al, 2021; Bertozzi et al, 2020).

Recently, authors from the control systems community have proposed the use of feedback control to mitigate the spread of the COVID-19 epidemic (Stewart et al, 2020). In that work, the authors use the SEIR model to show that a simple feedback law can manage the response to the pandemic for maximum survival while containing the damage to the economy. One approach to mitigate the spread of the disease while also trying to reduce economic shutdown is to control the numbers of hospitalized people to a desired number based on available hospital capacity. This ensures that the hospital system is not overwhelmed while avoiding unnecessary shutdowns (Stewart et al, 2020; Pazos, & Felicioni, 2020). Another approach to mitigation is through the recognition of a parameter R_0 called the basic reproduction parameter (Dolbeault, & Turinici, 2020). It has been shown in multiple papers using the SEIR dynamics that a value of $R_0 < 1$ ensures that the disease

10.1016/j.ifacol.2021.11.183

decreases in the population and in fact reduces exponentially fast (Bertozzi et al, 2020; Pazos, & Felicioni, 2020; Dolbeault, & Turinici, 2020). Recent papers have proposed the control of R_0 to a value below 1 as the approach to modulate disease spread prevention measures (Stewart et al, 2020).

Our paper develops an observer to estimate the value of R_0 in real-time. Previous papers had assumed that the value of R_0 was available for feedback (Stewart et al, 2020), while in fact the typically available measured variables are only the number of diagnosed infections, number of hospitalizations and number of deaths. The importance of this work is that an ability to estimate the real-time value of the reproduction parameter R_0 can assist both the analysis of the disease spread numbers as well as the modulation of mitigation measures to bring the disease evolution dynamics into a stable reducing region.

The outline of the rest of this paper is as follows. Section 2 develops a dynamic model for the COVID-19 disease spread dynamics. A cascaded observer design to estimate both the states and the basic reproduction number is introduced in Section 3. The estimated results using the observer for the disease spread dynamics in Minnesota are then presented in Section 4. Section 5 presents the conclusions.

2. INFECTIOUS DISEASE DYNAMIC MODEL

2.1 Proposed Model

A generalized SEIR model enhanced with additional states is used to describe the dynamic system governing the infectious disease spread dynamics. The system equations can be expressed as:

$$\frac{dS}{dt} = -\frac{\beta S(t)\mu I(t)}{N} \tag{1}$$

$$\frac{dE}{dt} = \frac{\beta S(t)\mu I(t)}{N} - \alpha E(t) \tag{2}$$

$$\frac{dI}{dt} = \frac{\alpha E(t)}{\mu} - \gamma I(t) - \epsilon I(t) \tag{3}$$

$$\frac{dH}{dt} = \epsilon\mu I(t) - \rho_{rec} H(t) - \rho_{ICU} H(t) + q_{imp} Z(t) \tag{4}$$

$$\frac{dZ}{dt} = \rho_{ICU} H(t) - q_{imp} Z(t) - q_{death} Z(t) \tag{5}$$

$$\frac{dR}{dt} = \gamma\mu I(t) + \rho_{rec} H(t) \tag{6}$$

$$\frac{dD}{dt} = q_{death} Z(t) \tag{7}$$

This generalized model includes seven states: Susceptible population (*S*), Exposed population (*E*), detected Infected population (*I*), number of patients in Hospital but not in ICU (*H*), number of patients in ICU (*Z*), infected population who have recovered (*R*), and infected population who have passed away (*D*). It is assumed that the summation of these states will be equal to the total population (*N*).

$$S + E + I + H + Z + R + D = N \tag{8}$$

This generalized model, since it has more states and measurements compared to traditional SEIR models, will result in a more accurate and reliable estimation of the system (Peng et al, 2020). Note that, this model is nonlinear and requires more than simple linear observer design schemes for estimating its states.

The model parameters which determine the epidemic dynamics include the infection rate (β), inverse of average latent time (α), cure rate (γ), hospitalization rate (ϵ), recovery rate (ρ_{rec}), ICU rate (ρ_{ICU}), and mortality rate (q_{death}). Our generalized SEIR model also proposes a new parameter (μ) which signifies the ratio between the real and detected infected population.

$$I_{true} = \mu\, I \tag{9}$$

This relationship accounts for the difference between the total infected and the diagnosed population.

Assumptions: Though the current model is more sophisticated than the traditional SEIR model, some simplifying assumptions are still made. These include:

- The studied population is isolated from neighboring populations.
- The insusceptible population (the patients who have recovered from the disease) is considerably smaller than the total population.
- The number of patients in need of hospitalization or ICU beds does not exceed the capacity of the healthcare system.

2.2 Minnesota Data

To train the model and determine its parameters, a six-month data set (Minnesota Department of Health, 2020) was considered. This data includes numbers of infected, hospitalized, ICU admissions, recovered, and deaths. In other words, we have five of the seven states as measurements. The publicly reported date starts from March 21st of 2020 and ends on August 27th of 2020.[1]

2.3 Least-Squares Parameter Determination

To find the model parameters, it is necessary to notice that some parameters change over time and we cannot fit constant parameters for the whole time period. Specifically, the infection rate β changes due to social distancing orders and the parameters ϵ and μ vary due to increase in testing. Hence, we adopted the approach to divide the time domain into piecewise

[1] It is to be noted that after this date the style of the reported data changed, and the new style was not compatible with the model used in this paper.

periods of time and keep these three parameters constant in each piecewise period to achieve an acceptable fitted model.

To this end, the second derivative of the infected population state I was used to split the time domain into piecewise intervals. The reasoning behind this strategy is that, as can be inferred from (2) and (3), the parameter β is related to the second derivative of I. Specifically, by combining (2) and (3) we have:

$$\frac{\partial^2 I}{\partial t^2} = \beta\left(\frac{\alpha SI}{N}\right) + other\ terms$$

Hence, a considerable change in $\frac{\partial^2 I}{\partial t^2}$ can be equivalent to a significant change in β. Accordingly, to find the numerical value of $\frac{\partial^2 I}{\partial t^2}$, a second order forward finite difference scheme was used:

$$f''(x) = \frac{f(x+2h) - 2f(x+h) + f(x)}{h^2} \qquad (10)$$

The result is shown in Fig. 1. As can be seen in this figure, the time domain is roughly divided into regions with positive and negative signs (as a measure for classifying large changes) of $\frac{\partial^2 I}{\partial t^2}$. The piecewise time periods with constant parameters, hence, were chosen as [0-35], [35-70], [70-105], and [105-160] days after March 21st.

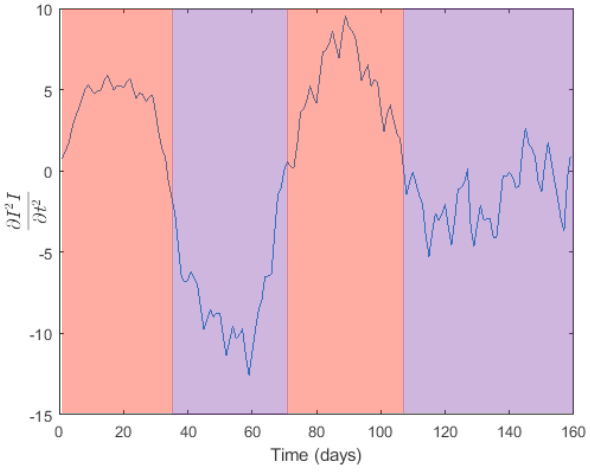

Fig. 1. The time domain is divided based on the sign of the second derivative of infected population.

To fit the model using all of the existing data set, a least-squares method was utilized (D'Errico, 2012). To improve the fitting, different weights were used for the different variables. Since the values of H and Z are much smaller than the other states, a higher weight was given to them ($W_i = 10$). Additionally, since R is not going to be utilized in the observer design, a smaller weight was chosen for it ($W_i = 0.01$).

Furthermore, since the incubation period has been reported to be between 2 to 14 days (Yang et al, 2020), it was assumed that the average latent time is within the interval of $\alpha^{-1} \in [0.1,0.2]$. The resulting model along with the actual data is presented in Figs. 2-5. As can be seen, the generalized SEIR model accurately reconstructs the data. The susceptible state is also presented in Fig.6. As can be seen in the figure, as more of the population gets infected, the susceptible population decreases.

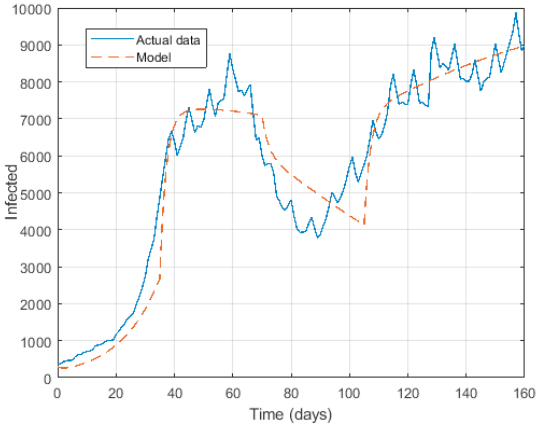

Fig. 2. The fitted model of the infected population and infected numbers from the data

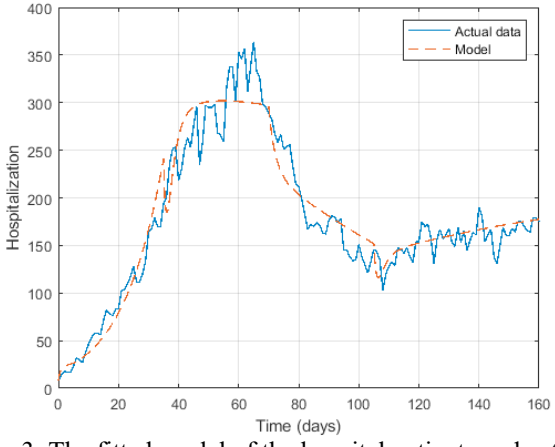

Fig. 3. The fitted model of the hospital patients and actual hospitalization numbers

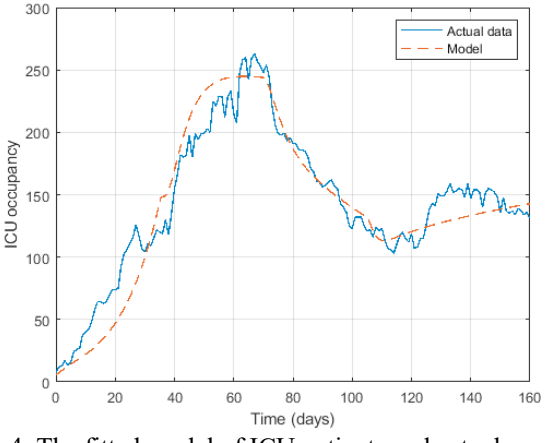

Fig. 4. The fitted model of ICU patients and actual patients admitted to ICU

The resulting parameters of the model are presented in Table. 1. As was stated, all the parameters are kept constant for the whole time except for parameters β, ϵ, and, μ which were constant in each piecewise interval. As can be seen, the infection rate β decreases after the first time period due to the

Minnesota's stay-at-home order on March 27th. The effect of increase in prevalence of COVID testing also can be seen in reduction of μ after the first 35 days.

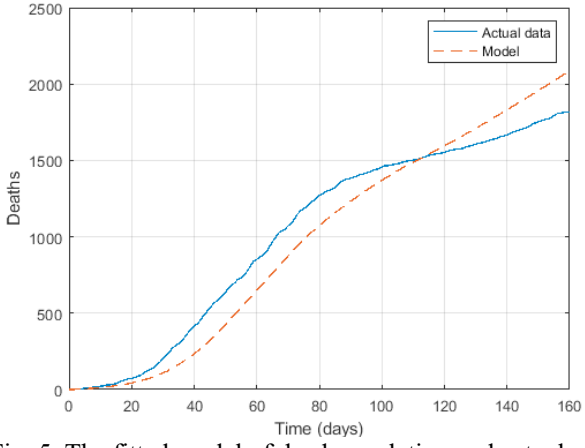

Fig. 5. The fitted model of dead population and actual number of deaths

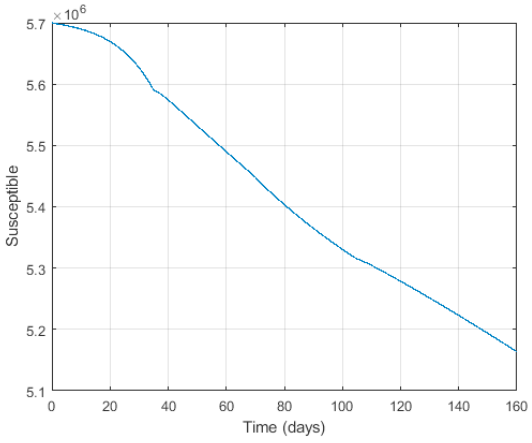

Fig. 6. Susceptible population according to the model

3. CASCADED OBSERVER DESIGN

The design of the overall estimation system is motivated by the following aspects of the dynamic system:

i) Since H, Z, and D are measured, equations (4), (5), and (7) can be used to estimate μ.

ii) Once μ is known, with a known I_{true} , the infection rate β can be estimated using (1) and (2).

In consequence, a cascaded observer is used to estimate the infection rate and eventually R_0. The first observer uses the measurements of H, Z,and D as states and I as input to create an estimate for μ. Then by utilizing μ, the true infected population number is calculated, and the infection rate β is estimated. A schematic of the cascaded observer is presented in Fig. 7.

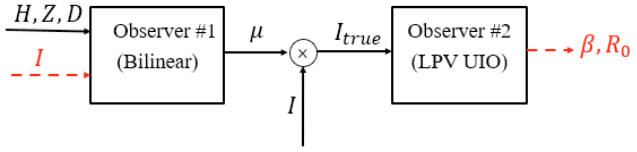

Fig. 7. Schematic of cascaded observer

Table 1. System parameters

Parameters	0-35 days	35-70 days	70-105 days	105-160 days
γ	0.2388	same	same	same
β	0.4534	0.2619	0.2378	0.2846
ϵ	0.0125	0.0166	0.0100	0.0139
ρ_{rec}	0.8409	same	same	same
ρ_{ICU}	0.1666	same	same	same
q_{imp}	0.1116	same	same	same
q_{death}	0.0925	same	same	same
α	0.1969	same	same	same
μ	7.2959	2.3050	3.3045	1.3081

3.1 Bilinear Observer

To estimate the ratio μ between actual and detected infected population, we consider it to be a state and assume its derivative to be zero.

$$\frac{d\mu}{dt} = 0 \tag{11}$$

Using (4), (5), (7), and (11), the system for observer #1 is in the following bilinear form (Elliott, 2009):

$$\begin{aligned} \dot{x} &= Ax + Bxu \\ y &= Cx \end{aligned} \tag{12}$$

where the states are $x = [H, Z, D, \mu]^T$, the input $u = I$,

$$A = \begin{bmatrix} -\rho_{ICU} - \rho_{rec} & q_{imp} & 0 & 0 \\ \rho_{ICU} & -q_{imp} - q_{death} & 0 & 0 \\ 0 & q_{death} & 0 & 0 \\ 0 & 0 & 0 & 0 \end{bmatrix},$$

$$B = \begin{bmatrix} 0 & 0 & 0 & \epsilon \\ 0 & 0 & 0 & 0 \\ 0 & 0 & 0 & 0 \\ 0 & 0 & 0 & 0 \end{bmatrix}, \text{ and } C = \begin{bmatrix} 1 & 0 & 0 & 0 \\ 0 & 1 & 0 & 0 \\ 0 & 0 & 1 & 0 \end{bmatrix}.$$

Let the state observer be given by:

$$\dot{\hat{x}} = A\hat{x} + B\hat{x}u + L(y - C\hat{x}) \tag{13}$$

Let the estimation error be $\tilde{x} = x - \hat{x}$. The estimation error dynamics then can be found by subtracting (13) from (12):

$$\dot{\tilde{x}} = (A + Bu - LC)\tilde{x} \tag{14}$$

Note that due to the bilinear nature of the system, the closed-loop matrix in (14) is a function of the known input u.

Theorem 1. If the Linear Matrix Inequalities (15) have a feasible solution, the resulting observer gain L guarantees that the observer (13) is globally exponentially stable. Here $P > 0$ is a positive definite matrix and u_{min} and u_{max} are the lower

and upper bound on the input ($u_{min} < u < u_{max}$), and σ is a diagonal matrix that determines the convergence rate.

$$\begin{aligned}&(A + Bu_{max} - LC)^T P + P(A + Bu_{max} - LC)\\&+ \sigma P\sigma \le 0\\&(A + Bu_{min} - LC)^T P + P(A + Bu_{min} - LC)\\&+ \sigma P\sigma \le 0\end{aligned} \tag{15}$$

Proof. Consider $V = \frac{1}{2}x^T Px$ as the candidate for the Lyapunov function, with $P > 0$. By utilizing (14) the derivative of Lyapunov function will be:

$$\begin{aligned}\dot{V} &= \dot{\tilde{x}}^T P\tilde{x} + \tilde{x}^T P\dot{\tilde{x}}\\&= \tilde{x}^T(A + Bu - LC)^T P\tilde{x} + \tilde{x}^T P(A + Bu - LC)\tilde{x}\end{aligned}$$

To guarantee stability, $\dot{V} \le 0$ could be ensured. To achieve exponential stability $\dot{V} + \tilde{x}^T\sigma P\sigma\tilde{x} \le 0$ can be used instead, where $\sigma > 0$ and is defined as:

$$\sigma = \begin{bmatrix}\sigma_1 & 0 & 0 & 0\\0 & \sigma_2 & 0 & 0\\0 & 0 & \sigma_3 & 0\\0 & 0 & 0 & \sigma_4\end{bmatrix} \tag{16}$$

The convergence rate in this case will be at least equal to $\frac{\min(\sigma_i^2)\lambda_{min}(P)}{2}$ where $\lambda_{min}(.)$ denotes the minimum eigenvalue of the matrix.

Hence, the LMI to be satisfied will be:

$$\begin{aligned}&(A + Bu - LC)^T P + P(A + Bu - LC) + \sigma P\sigma\\&\le 0\end{aligned} \tag{17}$$

Any control input $u(t)$, $u_{min} \le u(t) \le u_{max}$, can be expressed as

$$u(t) = \delta u_{min} + (1 - \delta)u_{max}, \qquad 0 \le \delta \le 1 \tag{18}$$

with time-varying δ.

Using (18), LMI (17) can be written as:

$$\begin{aligned}&\delta[(A + Bu_{min} - LC)^T P + P(A + Bu_{min} - LC) + \sigma P\sigma] +\\&(1 - \delta)[(A + Bu_{max} - LC)^T P + P(A + Bu_{max} - LC) +\\&\sigma P\sigma] \le 0\end{aligned}$$

Hence, if both LMIs in (15) are satisfied, the constant solution P and the resulting gain L will ensure that the observer (13) is globally exponentially stable.

3.2 Unknown Input Observer for a Linear Parameter Varying system

To estimate the infection rate, we start with (2) and (3). If it is assumed that $S \approx N$ (the susceptible population is very large compared to the other states), then using (9) the system will be:

$$\begin{aligned}\frac{dE}{dt} &= \beta I_{true} - \alpha E\\\frac{d\,I_{true}}{dt} &= \alpha E - \gamma I_{true} - \epsilon I_{true}\end{aligned} \tag{19}$$

The system, therefore, can be expressed as:

$$\begin{aligned}\dot{x} &= Ax + D_\rho\, d\\y &= Cx\end{aligned} \tag{20}$$

where $x = [\,E\ I_{true}]^T, A = \begin{bmatrix}0 & -\alpha\\\alpha & \gamma + \epsilon\end{bmatrix}, C = [0\ 1],\ D_\rho = \begin{bmatrix}y\\0\end{bmatrix}$, and $d = \beta$ is an unknown input.

Theorem 2. The observer in the form of

$$\dot{\hat{x}} = \big(A - LC - Q_\rho M_{r\rho}\big)\hat{x} + Q_\rho y^{(r)} + Ly \tag{21}$$

is asymptotically stable and the estimate of the unknown input

$$\hat{d} = \big(M_{r-1}D_\rho\big)^{-1}\big(y^{(r)} - M_{r\rho}\hat{x}\big) \tag{22}$$

converges toward the true value if the eigenvalues of the matrix $(A - LC - Q_\rho M_{r\rho})$ are all negative. Where r is the relative degree of the system, $y^{(n)}$is the n^{th} derivative of the output, $Q_\rho = D_\rho\big(M_{r-1}D_\rho\big)^{-1}$, and $M_{i\rho}$can be calculated from

$$\begin{aligned}y^{(i)} &= M_{i\rho}x, && 1 \le i < r\\y^{(r)} &= M_{r\rho}x + M_{r-1}D_\rho d\,, && i = r\end{aligned} \tag{23}$$

Proof. (Ichalal, & Mammar, 2015; Vijayaraghavan et al, 2006)

4. ESTIMATION RESULTS

To use the first observer for the bilinear system and find μ, the convergence rate in (16) is chosen as $\sigma^2 = 10^{-3}\begin{bmatrix}5 & 0 & 0 & 0\\0 & 1000 & 0 & 0\\0 & 0 & 100 & 0\\0 & 0 & 0 & 10\end{bmatrix}$. By solving the LMIs (15) numerically using the YALMIP toolbox (Lofberg, 2004) the observer gain is found to be

$$L = \begin{bmatrix}20.26 & 35.11 & 49.34\\1.38 & 1.93 & 2.85\\1.51 & 2.54 & 3.49\\0.046 & 0.076 & 0.11\end{bmatrix}.$$

It is to be mentioned that the matrix B is dependent on ϵ, but ϵ changes in each piecewise interval. To deal with this problem, the gain is designed for one interval and is checked for other intervals to satisfy the feasibility of LMIs (15). The estimated value of the ratio between the actual and detected infected population along with its previous constant values from the least-squares method is presented in Fig. 8.

Resulting from (22), the estimate of infection rate can be calculated from:

$$\hat{\beta} = \left(CA\begin{bmatrix}I_{true}\\0\end{bmatrix}\right)^{-1}\big(\ddot{I}_{true} - CA^2\hat{x}\big) \tag{25}$$

where $\ddot{I}_{true}$is calculated numerically using (10). The gain $L = \begin{bmatrix}1.5\\1\end{bmatrix}$ satisfies the Theorem 1 for all the piecewise time intervals. The estimated infection rate β along with its constant values from the least-squares method is presented in Fig. 9.

In general, as can be seen in Fig. 9 and Fig. 10, the estimated real-time values μ and β match well with the least-squares values obtained from the complete data set. However, the

observer estimates do vary more with time than the least-squares results. To find the basic production number, the following equation is used.

$$R_0 = \frac{\beta}{\epsilon + \gamma} \tag{26}$$

The resulting estimate of R_0 is presented in Fig. 10. As can be seen in Fig. 10, not only the result of social distancing order from March 27th is visible[2], but also the increase of R_0 as a result of loosening of the restrictions on May 18th (day 58 in the figure)[3] by "Safely Reopening Minnesota's Economy" is also detectable. The mass demonstrations during the summer of 2020 could also have had an effect in increase of R_0 between May 26th and June 7th (days 66-78 of Fig. 10). The decline in R_0 around the day 90 could be a result of decrease in the protests (Ran et al, 2021; Valentine et al, 2020). It needs to be mentioned that the correlation between the social protests and the rise in COVID-19 spread is questioned in multiple works (Gonsalves, & Yamey, 2020; Lazer et al, 2021) and is not a specific claim that this work makes.

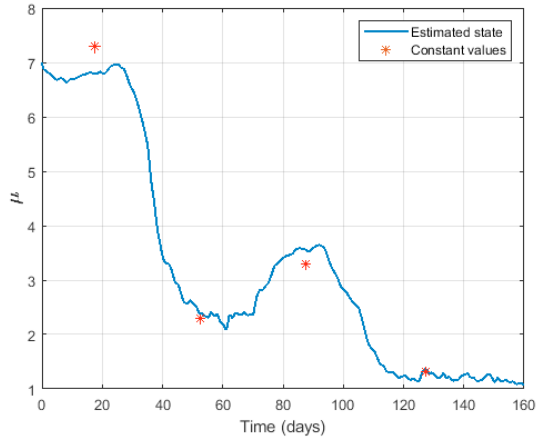

Fig. 8. Ratio between the actual and detected infected population.

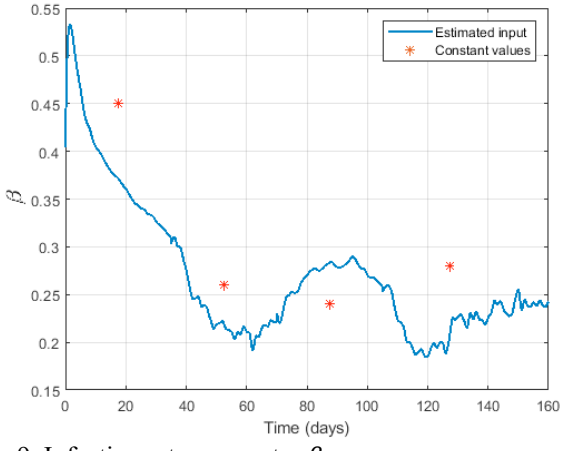

Fig. 9. Infection rate parameter β

5. CONCLUSIONS

This paper considered the dynamics of the COVID-19 pandemic and real-time estimation of the basic reproduction number as a key variable for controlling the spread of the disease. By adding variables on hospitalizations, ICU admissions, and number of deaths, a nonlinear generalized SEIR model was developed. A least-squares method was utilized to find the parameters of the system based on the complete data set of 6-month statistics published by the Minnesota Department of Health.

A cascaded observer system, consisting of a bilinear observer and an unknown input observer, was used to estimate the real-time values of the true infected population, the infection rate, and the basic reproduction number.

The resulting real-time estimates matched well with the least-squares values obtained from the whole data set. The real-time estimates provide timely information and could be utilized to control the spread of the disease. For instance, the reproduction number could be controlled to a value below 1 by fine-tuning social distancing measures and lock-downs, so that economic pain is minimized while the disease dynamics are still maintained to be in a stable region.

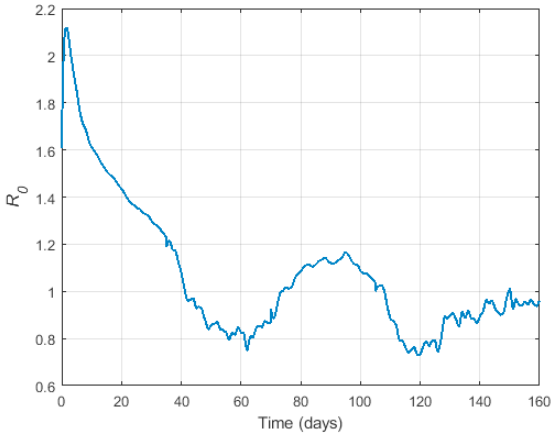

Fig. 10. Basic reproduction number

REFERENCES

Bertozzi, A.L., Franco, E., Mohler, G., Short, M.B. and Sledge, D., 2020. The challenges of modeling and forecasting the spread of COVID-19. *Proceedings of the National Academy of Sciences*, *117*(29), pp.16732-16738.

Chen, L. and Sun, J., 2014. Global stability of an SI epidemic model with feedback controls. *Applied Mathematics Letters*, *28*, pp.53-55.

D'Errico, J., 2012. fminsearchbnd, fminsearchcon–File Exchange–MATLAB Central.

De la Sen, M., Ibeas, A., Alonso-Quesada, S. and Nistal, R., 2017. On a new epidemic model with asymptomatic and dead-infective subpopulations with feedback controls useful for Ebola disease. *Discrete dynamics in Nature and society*, *2017*.

[2] State of Minnesota Executive Department. (2020, March 25). Emergency executive order 20–20.

[3] State of Minnesota Executive Department. (2020, May 13). Emergency executive order 20–56.

De Wit, E., Van Doremalen, N., Falzarano, D. and Munster, V.J., 2016. SARS and MERS: recent insights into emerging coronaviruses. *Nature Reviews Microbiology*, *14*(8), p.523.

Dolbeault, J. and Turinici, G., 2020. Heterogeneous social interactions and the COVID-19 lockdown outcome in a multi-group SEIR model. *Mathematical Modelling of Natural Phenomena*, *15*, p.36.

Elliott, D., 2009. *Bilinear control systems: matrices in action* (Vol. 169). Springer Science & Business Media.

Gonsalves, G. and Yamey, G., 2020. Political interference in public health science during covid-19, *BMJ*, 371, pp. 19-20

Hethcote, H.W. and Van den Driessche, P., 1991. Some epidemiological models with nonlinear incidence. *Journal of Mathematical Biology*, *29*(3), pp.271-287.

Ichalal, D. and Mammar, S., 2015. On unknown input observers for LPV systems. *IEEE Transactions on Industrial Electronics*, *62*(9), pp.5870-5880.

Lazer, D., Santillana, M., Perlis, R.H., Ognyanova, K., Baum, M., Druckman, J., Quintana, A., Volpe, J.D., Chwe, H., Simonson, M., 2021. The COVID States Project #10: The pandemic and the protests. doi:10.31219/osf.io/qw43g.

I. Lofberg, J., 2004, September. YALMIP: A toolbox for modeling and optimization in MATLAB. In *2004 IEEE international conference on robotics and automation* (pp. 284-289). IEEE.

Lopman, B., Liu, C.Y., Le Guillou, A., Handel, A., Lash, T.L., Isakov, A.P. and Jenness, S.M., 2021. A modeling study to inform screening and testing interventions for the control of SARS-CoV-2 on university campuses. *Scientific Reports*, *11*(1), pp.1-11.

Minnesota Department of Health, 2020. Situation Update for COVID-19. https://www.health.state.mn.us/diseases/coronavirus/situation.html.

Pazos, F.A. and Felicioni, F., 2020. A control approach to the Covid-19 disease using a SEIHRD dynamical model. *medRxiv*.

Peng, L., Yang, W., Zhang, D., Zhuge, C. and Hong, L., 2020. Epidemic analysis of COVID-19 in China by dynamical modeling. *arXiv preprint arXiv:2002.06563*.

Ran, J., Zhao, S., Han, L., Chong, M.K., Qiu, Y., Yang, Y., Wang, J., Wu, Y., Javanbakht, M., Wang, M.H. and He, D., 2021. The changing patterns of COVID-19 transmissibility during the social unrest in the United States: A nationwide ecological study with a before-and-after comparison. *One Health*, *12*, p.100201.

Stewart, G., Heusden, K. and Dumont, G.A., 2020. How control theory can help us control COVID-19. *IEEE Spectrum*, *57*(6), pp.22-29.

Valentine, R., Valentine, D. and Valentine, J.L., 2020. Relationship of George Floyd protests to increases in COVID-19 cases using event study methodology. *Journal of Public Health*, *42*(4), pp.696-697.

Vijayaraghavan, K., Rajamani, R. and Bokor, J., 2006, June. Quantitative fault estimation for a class of nonlinear systems. In *2006 American Control Conference* (pp. 6-pp). IEEE.

Yang, Z., Zeng, Z., Wang, K., Wong, S.S., Liang, W., Zanin, M., Liu, P., Cao, X., Gao, Z., Mai, Z. and Liang, J., 2020. Modified SEIR and AI prediction of the epidemics trend of COVID-19 in China under public health interventions. *Journal of thoracic disease*, *12*(3), p.165.

Zhong, L., Mu, L., Li, J., Wang, J., Yin, Z. and Liu, D., 2020. Early prediction of the 2019 novel coronavirus outbreak in the mainland China based on simple mathematical model. *IEEE Access*, *8*, pp.51761-51769.